Copy No._____

DEFENCE R&D DÉFENSE

RANS calculations of the evolution of vortices

David Hally

George D. Watt

Defence R&D Canada

Technical Report

DREA TR 2001-216

May 2002

National Defence Défense nationale

Canada

104-06982/

RANS calculations of the evolution of vortices

David Hally

George D. Watt

Defence R&D Canada – Atlantic

Technical Report

DREA TR 2001-216

May 2002

Author

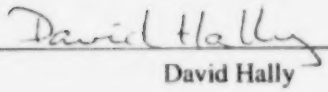

David Hally

Approved by

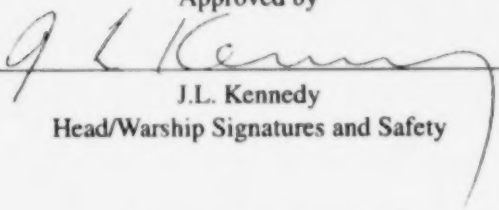

J.L. Kennedy
Head/Warship Signatures and Safety

Approved for release by

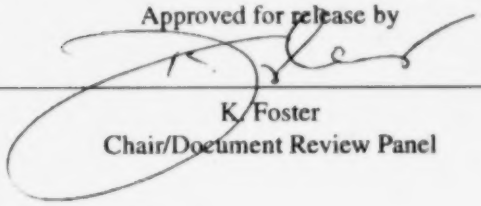

K. Foster
Chair/Document Review Panel

© Her Majesty the Queen as represented by the Minister of National Defence, 2002

© Sa majesté la reine, représentée par le ministre de la Défense nationale, 2002

Abstract

The evolution of a laminar vortex was calculated using the Reynolds-averaged Navier-Stokes solvers TRANSOM and CFX-TASCflow. Calculations were done on grids of varying density and were compared to an approximate solution of the Navier-Stokes equation. Both solvers generated accurate predictions for this flow. The solutions were used to make recommendations for the grid density required for accurate predictions of the pressure in the core as the vortex evolves over hundreds of core diameters.

TRANSOM was also used to determine the effect of grid density on a turbulent vortex, though in this case there is no analytic solution for comparison.

Résumé

Nous avons calculé l'évolution d'un tourbillon laminaire à l'aide des solutionneurs TRANSOM et CFX-TASCflow de l'équation de Navier-Stokes moyennée – ou RANS pour Reynolds-averaged Navier-Stokes. Nous avons comparé les calculs faits sur des maillages de densités différentes avec une solution approximative de l'équation de Navier-Stokes. Les solutionneurs ont tous deux donné des prédictions précises pour cet écoulement. Nous avons utilisé ces prédictions pour faire des recommandations sur la densité minimum du maillage permettant de prédire précisément la pression au cœur du tourbillon, alors que celui-ci évolue sur des dimensions supérieures à plusieurs centaines de diamètres du cœur.

Nous avons aussi utilisé TRANSOM pour déterminer l'effet de la densité du maillage en un tourbillon turbulent, bien que, pour ce cas, nous ne disposions pas de solution analytique permettant de faire une comparaison.

This page intentionally left blank.

Executive summary

Background

The Warship Signatures and Safety Section at DREA wishes to apply Reynolds-averaged Navier-Stokes (RANS) solvers to the prediction of vortices generated by ships, submarines and propellers. One question of interest is how dense the grid must be in the vortex core in order to model the pressure adequately. The answer will have an important effect on the gridding strategy used when modelling marine vortices.

Principal results

The evolution of a laminar vortex was calculated using the RANS solvers TRANSOM, developed at DREA, and CFX-TASCflow, developed by AEA Technology Ltd. There is an approximate solution to the Navier-Stokes equations which describes the vortex. This flow provides both a verification case for vortex-like flows and an opportunity for testing the effect of grid density on the solution.

The flow was solved on grids of varying density. Both TRANSOM and CFX-TASCflow generated accurate solutions to the flow even on sparse grids. TRANSOM was also used to determine the effect of grid density on a turbulent vortex, though in this case there is no analytic solution for comparison.

It is estimated that a minimum of five or six grid cells across the core is required to model the pressure adequately for predicting cavitation inception. Ten cells across the core would be preferable.

Significance of results

These calculations indicate that both CFX-TASCflow and TRANSOM can predict vortex-like flows accurately. The estimates of minimum grid density will be used when formulating gridding strategies for vortices on propellers.

Future work

The calculations reported here are a preliminary step in an on-going research effort to predict tip and leading edge vortex cavitation on marine propellers. The next step is to develop a strategy for generating grids capable of resolving the vortices adequately. Then an investigation of appropriate turbulence models will be begun.

David Hally, George D. Watt; 2002; RANS calculations of the evolution of vortices; DREA TR 2001-216; Defence R&D Canada – Atlantic.

Sommaire

Contexte

La section Signatures et sécurité des navires du CRDA désire utiliser des solutionneur de l'équation de Navier-Stokes moyennée – ou RANS pour Reynold-averaged Navier-Stokes – pour prédire les tourbillons générés par des navires, des sousmarins et des hélices marines. Une question importante est : quelle densité le maillage du calcul au cœur du tourbillon devra-t-il avoir pour modéliser correctement la pression ? La réponse à cette question aura un impact important sur la stratégie de maillage lorsque l'on voudra modéliser les tourbillons provoqués par les navires, les sousmarins, et les hélices.

Résultats principaux

On a calculé l'évolution du tourbillon laminaire à l'aide des solutionneurs TRANSOM, mis au point au CRDA, et CFX-TASCflow produit de AEA Technology Ltd. Il existe une solution approximative des équations de Navier-Stokes qui décrivent le tourbillon. Cet écoulement nous donne un point de contrôle pour les écoulements analogues au tourbillon et la possibilité de tester l'effet de la densité du maillage sur la solution.

Nous avons résolu l'écoulement à partir de maillages de densités différentes. Les logiciels TRANSOM et CFX-TASCflow ont tous deux produit des solutions possibles pour l'écoulement, même pour un maillage clairsemé. Nous avons utilisé TRANSOM pour établir les effets de la densité du maillage pour un tourbillon turbulent, bien que, dans ce cas, il n'existe pas de solution analytique permettant une comparaison.

Pour modéliser correctement la pression et prédire l'apparition de cavitation, on estime qu'un minimum de cinq ou six cellules du maillage doivent couvrir le cœur. Une couverture de dix cellules serait préférable.

Importance des résultats

Ces calculs nous indiquent que CFX-TASCflow et TRANSOM peuvent prédire avec précision les écoulements tourbillonnants. Nous utiliserons ces estimations du maillage minimum lorsque nous établirons les stratégies de maillage pour les tourbillons causés par les hélices.

Travaux à venir

Les calculs décrits dans ce rapport constituent une étape préliminaire d'une recherche en cours dont l'objectif est la prédiction de la cavitation causée par les tourbillons au bout et sur le bord d'attaque des pales des hélices marines. La prochaine étape est la production d'une stratégie de production d'un maillage capable de résoudre correctement les tourbillons. La recherche sur les modèles appropriés pour la turbulence pourra alors commencer.

David Hally, George D. Watt ; 2002 ; RANS calculations of the evolution of vortices ; DREA TR 2001-216 ; R&D pour la défense Canada – Atlantique.

This page intentionally left blank.

Table of contents

Abstract i

Résumé i

Executive summary iii

Sommaire iv

Table of contents vii

List of figures viii

1 Introduction 1

2 The evolution of a laminar vortex 1

2.1 Theory 1

2.2 RANS calculations 3

2.3 The effect of the order of the TRANSOM convective terms . . 6

2.4 The effect of the TRANSOM pseudo-compressibility constant 8

3 The evolution of a turbulent vortex 10

4 Concluding remarks 15

References 16

Distribution List 17

List of figures

1 The coordinate system 2

2 Velocity in the downstream plane; three cells across the vortex core. . 3

3 Velocity in the downstream plane; six cells across the vortex core. . . 3

4 Pressure in the upstream and downstream planes; three cells across the vortex core. 5

5 Pressure in the upstream and downstream planes; six cells across the vortex core. 5

6 Pressure in the upstream and downstream planes; ten cells across the vortex core. 5

7 Pressure in the vortex core; three cells across the vortex core. 7

8 Pressure in the vortex core; six cells across the vortex core. 7

9 Pressure in the vortex core; ten cells across the vortex core. 7

10 Radial velocity of all points in the downstream plane; three cells across the vortex core. 7

11 Radial velocity of all points in the downstream plane; six cells across the vortex core. 7

12 Radial velocity of all points in the downstream plane; ten cells across the vortex core. 7

13 Velocity deficit in the core; three cells across the vortex core. 8

14 Velocity deficit in the core; six cells across the vortex core. 8

15 Velocity deficit in the core; ten cells across the vortex core. 8

16 Velocity deficit in the core; 22 cells across the vortex core. 8

17 Solutions with flux difference order one; cells across the core from 3 to 22. 9

18 Solutions with flux difference order three; cells across the core from 3 to 22. 9

19 Solutions with flux difference order five; cells across the core from 3 to 10. 9

20 Solutions with β varying from 0.0001 to 100; three cells across the core. 11

21 Solutions with β varying from 0.0001 to 100; six cells across the core. 11

22 Velocity deficit in the core with β varying from 0.01 to 100; three cells across the core. 11

23 Velocity deficit in the core with β varying from 0.01 to 100; six cells across the core. 11

24 Turbulent vortex: velocity and turbulent viscosity in the downstream plane. 13

25 Turbulent vortex: pressure in the upstream and downstream planes. . . 13

26 Turbulent vortex: turbulent viscosity and pressure in the vortex core. . 13

27 The effect of the order of the turbulence model convective terms: Pressure and turbulent viscosity at the downstream plane. 14

28 The effect of the order of the turbulence model convective terms: Pressure and turbulent viscosity in the vortex core. 14

29 Turbulent viscosity at the downstream plane. 14

30 Turbulent viscosity in the vortex core. 14

1 Introduction

The Warship Signatures and Safety Section at DREA wishes to apply Reynolds-averaged Navier-Stokes (RANS) solvers to the prediction of vortices generated by ships, submarines and propellers. Important applications are the prediction of tip and leading edge vortex cavitation on propellers, of keel and body vortices which can influence propeller efficiency and underwater vehicle maneuvering characteristics, and of low aspect ratio appendage wake vortices which can compromise the performance of downstream control surfaces (for example, the influence of a submarine sail on its tailplanes).

As a preliminary test, the evolution of a laminar vortex was calculated using the RANS solvers TRANSOM[1], developed at DREA, and CFX-TASCflow[2], developed by AEA Technology Ltd. There is an approximate solution to the Navier-Stokes equations which describes the vortex making it a good verification case for the flow solvers.

Also of interest is the effect of the grid density on the solution. In particular, how many cells are necessary in the vortex core to model the pressure adequately? The dependence on the grid will have an important effect on the gridding strategy used when modelling propeller vortices. The dependence on grid density was tested using the laminar vortex as well as with TRANSOM predictions of a turbulent vortex for which there is no analytical solution.

2 The evolution of a laminar vortex

2.1 Theory

First we note the following solution to the Navier-Stokes equations[3] in a cylindrical coordinate system, (x, r, θ) (see Figure 1):

$$v_x = U; \quad v_r = 0; \quad v_\theta = \frac{C}{2\pi r}\left(1 - e^{-\frac{r^2}{4\nu t}}\right); \quad p = \frac{\rho C^2}{4\pi^2}\int \frac{1}{r^3}\left(1 - e^{-\frac{r^2}{4\nu t}}\right)^2 dr \tag{1}$$

This is a decaying vortex with centre on the line $r = 0$, circulation C, fluid density ρ and kinematic viscosity ν.

In a convection dominated flow, t can be replaced by x/U to obtain an approximate solution for a steady vortex as it convects downstream:

$$v_x = U; \quad v_r = 0; \quad v_\theta = \frac{C}{2\pi r}\left(1 - e^{-\frac{Ur^2}{4\nu x}}\right); \quad p = \frac{\rho C^2}{4\pi^2}\int \frac{1}{r^3}\left(1 - e^{-\frac{Ur^2}{4\nu x}}\right)^2 dr \tag{2}$$

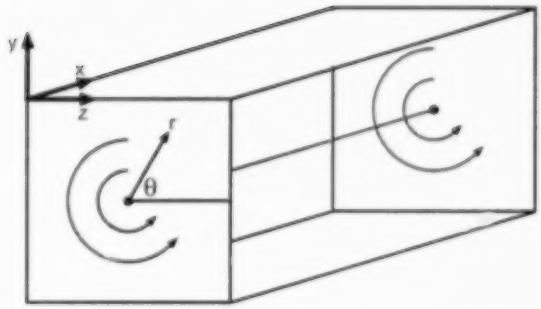

Figure 1: *The coordinate system*

Substituting this solution into the Navier-Stokes equations we find that the following terms, which were zero in the time dependent solution of Equation (1), are now non-zero; they must be small for the solution to be a good approximation.

$$-\frac{1}{\rho}\frac{\partial p}{\partial x} = \frac{C^2U}{8\pi^2\nu x^2}\int \frac{1}{r}\left(1-e^{-\frac{Ur^2}{4\nu x}}\right)e^{-\frac{Ur^2}{4\nu x}}dr \tag{3}$$

$$\nu\frac{\partial^2 v_\theta}{\partial x^2} = \frac{CUr(8\nu x - r^2U)}{32\pi\nu x^4}e^{-\frac{Ur^2}{4\nu x}} \tag{4}$$

Since

$$\int_0^\infty \frac{1}{r}\left(1-e^{-r^2}\right)e^{-r^2}dr = \frac{\ln 2}{2} \tag{5}$$

we can estimate the size of the first term by:

$$T_1 \equiv -\frac{1}{\rho}\frac{\partial p}{\partial x} \sim \frac{C^2U\ln 2}{16\pi^2\nu x^2} \approx 0.004\frac{C^2U}{\nu x^2} \tag{6}$$

The two terms in $\nu\partial^2 v_\theta/\partial x^2$ can be estimated from their maximum values over the radial distance r. Since

$$\max\left(re^{-\frac{Ur^2}{4\nu x}}\right) = \sqrt{\frac{2\nu x}{U}}\,e^{-\frac{1}{2}}; \quad \max\left(r^3e^{-\frac{Ur^2}{4\nu x}}\right) = \left(\frac{6\nu x}{U}\right)^{\frac{3}{2}}e^{-\frac{3}{2}}; \tag{7}$$

the two terms can be estimated by:

$$T_2 \sim \frac{Ce^{-\frac{1}{2}}}{2\pi}\sqrt{\frac{U\nu}{2x^5}} \approx 0.07\,C\sqrt{\frac{U\nu}{x^5}} \tag{8}$$

$$T_3 \sim -\frac{3Ce^{-\frac{3}{2}}}{16\pi}\sqrt{\frac{6U\nu}{x^5}} \approx 0.03\,C\sqrt{\frac{U\nu}{x^5}} \tag{9}$$

The convection term which is not small (it corresponds to the non-vanishing term $\partial v_\theta/\partial t$ in the time-dependent solution) is

$$T_4 \equiv u_x\frac{\partial v_\theta}{\partial x} = -\frac{CU^2r}{8\pi\nu x^2}e^{-\frac{Ur^2}{4\nu x}} \sim -\frac{Ce^{-\frac{1}{2}}}{8\pi}\sqrt{\frac{2U^3}{\nu x^3}} \approx -0.03C\sqrt{\frac{U^3}{\nu x^3}} \tag{10}$$

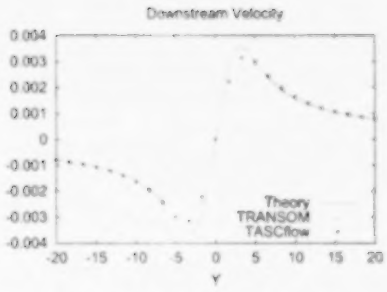

Figure 2: *Velocity in the downstream plane; three cells across the vortex core.*

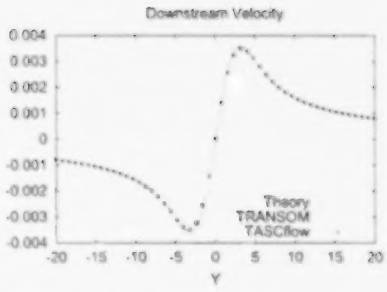

Figure 3: *Velocity in the downstream plane; six cells across the vortex core.*

For a valid approximation this term must be significantly larger than T_1, T_2 and T_3. We have $T_2, T_3 \ll T_4$ if

$$\frac{Ux}{\nu} \gg 1 \tag{11}$$

and $T_1 \ll T_4$ if

$$\frac{C}{\nu} \ll 10\sqrt{\frac{Ux}{\nu}} \tag{12}$$

If we define the radius of the vortex core to be the location of maximum v_θ, then

$$r_c \approx 2.24\sqrt{\frac{\nu x}{U}} \tag{13}$$

If r_c and U are used for the length and velocity scales, then the approximate solution is accurate when

$$\nu \ll \frac{r_c U}{2}; \qquad C \ll 4 r_c U \tag{14}$$

2.2 RANS calculations

TRANSOM and CFX-TASCflow were used to calculate the evolution of a laminar vortex using five grids of differing node density near the vortex core. Each of the grids was square in cross-section extending from $y = -20$ to 20 and from $z = -20$ to 20. The upstream plane is at $x = 1000$ and extends downstream to $x = 2000$.

Four of the grids had $N_x \times N_y \times N_z = 100 \times 51 \times 51$ nodes. The cross-stream spacing was adjusted near $(y, z) = (0, 0)$ so that there were roughly 6, 10, 16 and 22 grid cells across the vortex core. The downstream nodes were equally spaced. The fifth grid was similar to the other three but had $100 \times 25 \times 25$ nodes equally

spaced in all directions. This resulted in approximately three grid cells across the vortex core.

The velocity on the upstream plane was initialized using Equation (2) with $U = 1.0$, $\nu = 0.001$ and $C = 0.1$. On the outer boundaries the velocity was set according to Equation (2) for both solvers. In TRANSOM, the pressure gradient was set to zero at the downstream boundary; on the outer boundaries the pressure was set according to Equation (2). In TASCflow, the downstream boundary was an outlet; the outer boundaries were set to be inlets where the velocity in Equation (2) flowed inwards, outlets where it flowed outwards.

TRANSOM was run with a flux difference order of five and pseudo-compressibility constant 1.0 (see Sections 2.3 and 2.4 for descriptions of these parameters). CFX-TASCflow was run using its highest order discretization scheme, a pure second order linear profile skew advection scheme incorporating advection correction.

Figures 2 and 3 show the velocity in the downstream plane as predicted by Equation (2) and as calculated by TRANSOM and CFX-TASCflow for the grids with three and six cells across the vortex core. For the grids with more cells across the vortex core the calculated points are so close to the theoretical curve as to be indistinguishable from it.

For the three cell case, both programs perform well considering the lack of resolution of the vortex core. The CFX-TASCflow results are somewhat better than those of TRANSOM suggesting that it has lower levels of artificial dissipation. For the six cell case both programs match the theoretical curve very well.

Figures 4–6 show the pressure in the upstream and downstream planes. The theoretical curve was obtained by using the program Maple^{TM}[4] to integrate and then evaluate the expression for the pressure in Equation (2). In the downstream plane the TRANSOM and CFX-TASCflow results are comparable, both underpredicting the pressure drop somewhat. However, in the upstream plane the TRANSOM predictions are much better than those of CFX-TASCflow. Figures 7–9 show the pressure at $(y, z) = (0, 0)$ (the centre of the vortex) from the upstream to the downstream planes. These figures show clearly that there is a problem with the upstream boundary condition in CFX-TASCflow which causes it to misevaluate the pressure field over the first few nodes downstream.

In the downstream plane the pressure drop in the core is underpredicted by about 30% by both codes when there are three cells across the core. For six cells the underprediction reduces to about 6% and for ten cells to less than 1%.

A measure of the ability of the solvers to maintain the axisymmetric nature of the flow is shown in Figures 10–12. They plot the radial component of the velocity

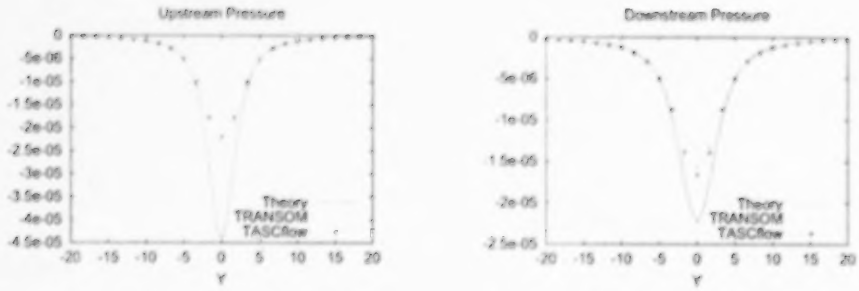

***Figure 4**: Pressure in the upstream and downstream planes; three cells across the vortex core.*

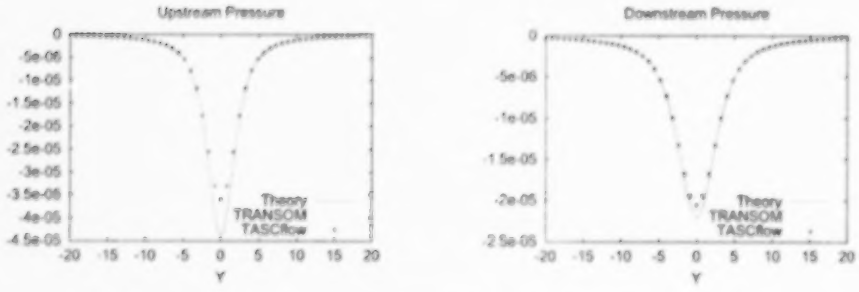

***Figure 5**: Pressure in the upstream and downstream planes; six cells across the vortex core.*

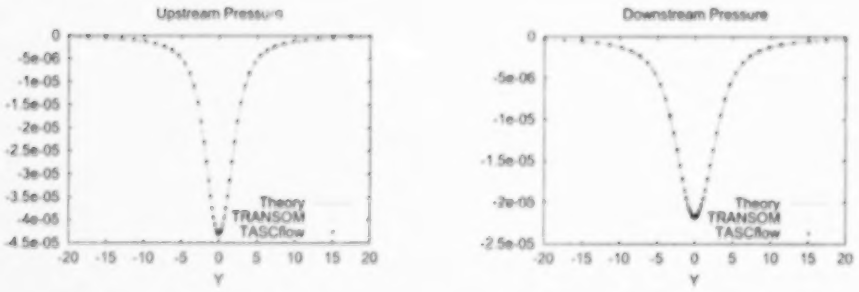

***Figure 6**: Pressure in the upstream and downstream planes; ten cells across the vortex core.*

versus distance from the core for every node in the downstream plane. For an axisymmetric solution these points should collapse to a single curve. The deviation from axisymmetry is similar for both codes though it is somewhat higher for TRANSOM in the three cell case. For TRANSOM, the maximum radial velocity normalized using the maximum azimuthal velocity is about 6% for the three cell case, about 1% for the six cell case, and about 0.3% for the ten cell case.

The change in v_x at the centre of the core can be approximated by assuming that the convective term in the x momentum equation is exactly balanced by the pressure term. This is a good approximation near the upstream plane but degrades downstream as the cross-stream variation of v_x becomes important. In this approximation the velocity deficit at the core is:

$$U - v_x(0,0) = U\left(\frac{C^2 \ln 2}{16\nu\pi^2}\frac{1}{x_0} - \frac{1}{x}\right) \tag{15}$$

The velocity deficit in the core is plotted in Figures 13–16. The numerical curves should be tangent to the theoretical curve at the left of the plot with the difference in the curves increasing with downstream distance.

TRANSOM performs somewhat better than CFX-TASCflow in these cases. The velocity deficit predicted by CFX-TASCflow is affected by the poor prediction for pressure in the upstream plane.

2.3 The effect of the order of the TRANSOM convective terms

To determine the effect of the flux difference order (the order of the finite difference approximations of the convective terms in the Navier-Stokes equations) on the TRANSOM solutions, the flow was recalculated using flux difference orders of one and three. The results are illustrated in Figures 17–19.

The results with a flux difference order of one are clearly completely unacceptable. Numerical dissipation causes the vortex to decay almost immediately. Increasing the number of cells past six across the vortex core has little effect; this suggests that the size of the cells in the streamwise direction is also important in this case.

With a flux difference order of three the results are much better, though even the most accurate solution (22 cells across the core) was inferior to the order five case with six cells across the core. It is also interesting to note that the 22 cell solution is not significantly different from the 16 cell solution, once again suggesting that downstream cell size is becoming important.

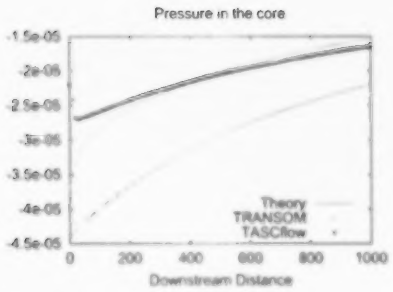

Figure 7: *Pressure in the vortex core; three cells across the vortex core.*

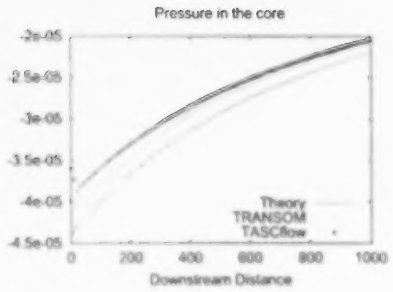

Figure 8: *Pressure in the vortex core; six cells across the vortex core.*

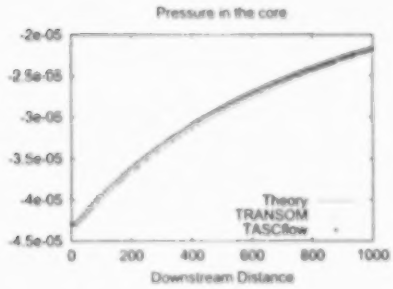

Figure 9: *Pressure in the vortex core; ten cells across the vortex core.*

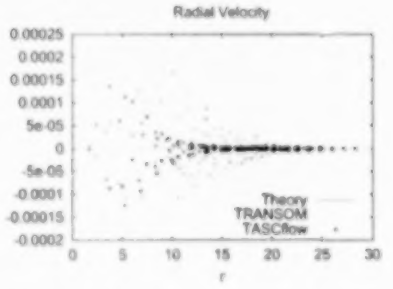

Figure 10: *Radial velocity of all points in the downstream plane; three cells across the vortex core.*

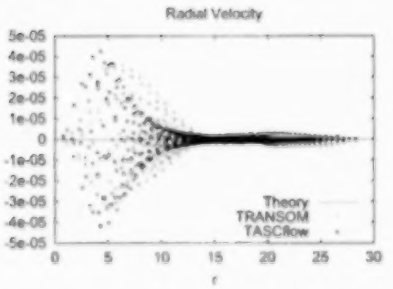

Figure 11: *Radial velocity of all points in the downstream plane; six cells across the vortex core.*

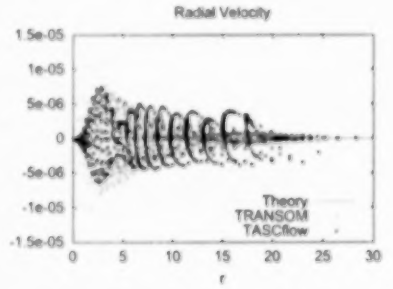

Figure 12: *Radial velocity of all points in the downstream plane; ten cells across the vortex core.*

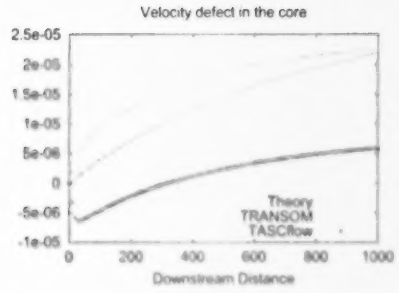

Figure 13: *Velocity deficit in the core; three cells across the vortex core.*

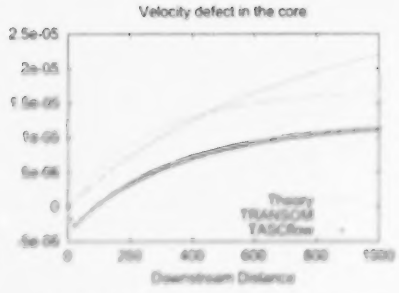

Figure 14: *Velocity deficit in the core; six cells across the vortex core.*

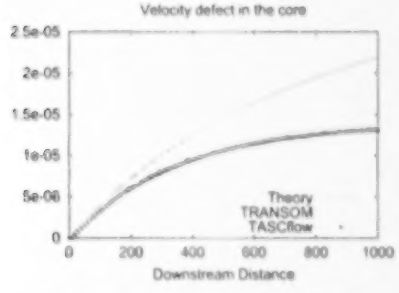

Figure 15: *Velocity deficit in the core; ten cells across the vortex core.*

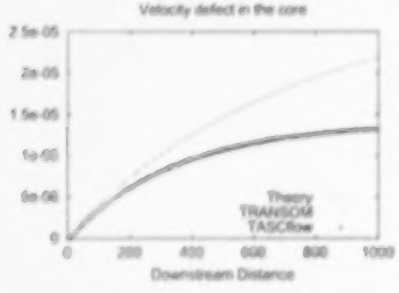

Figure 16: *Velocity deficit in the core; 22 cells across the vortex core.*

With a flux difference order of five excellent solutions are obtained with 10 cells across the core. Solutions with more cells have not been shown because their curves would not be discernible in the figures.

2.4 The effect of the TRANSOM pseudo-compressibility constant

TRANSOM uses a continuity equation which has the form:

$$\frac{1}{\rho\beta}\frac{\partial p}{\partial t} = \nabla \cdot \mathbf{v} \tag{16}$$

In theory, once a steady state solution has been reached, the pseudo-compressibility constant, β should have no effect. However, in the numerical solution, the value of β affects the characteristics along each of the coordinate directions and therefore it alters the numerical scheme for the convection and continuity terms.

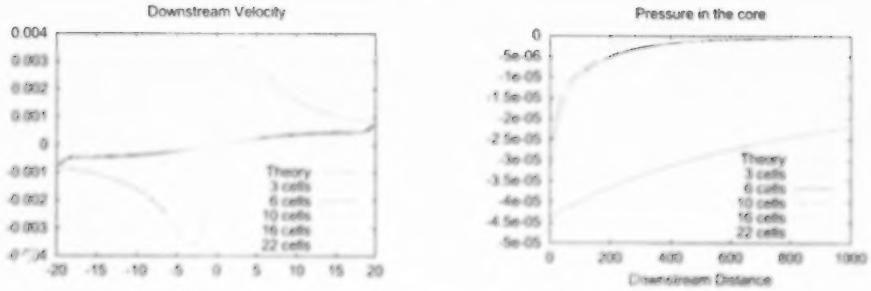

***Figure 17**: Solutions with flux difference order one; cells across the core from 3 to 22.*

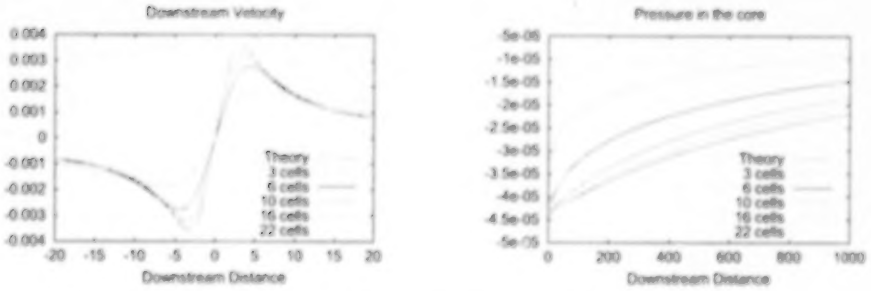

***Figure 18**: Solutions with flux difference order three; cells across the core from 3 to 22.*

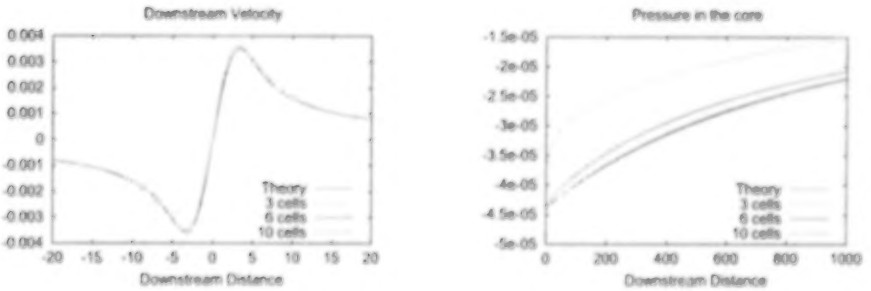

***Figure 19**: Solutions with flux difference order five; cells across the core from 3 to 10.*

Normally β, which has units of velocity squared, should be chosen to be the square root of a typical fluid velocity in the problem being solved. The current problem is unusual in that the cross-stream velocities, v_y and v_z, are several orders of magnitude smaller than the streamwise velocity, v_x. Therefore it is not clear which value of β is best.

To determine the effect of the pseudo-compressibility constant on the TRANSOM solutions, the flow was recalculated using values for β between 10^{-4} and 10^{2}. The results are shown in Figures 20–23.

As β decreases, the prediction of the transverse velocity field and the pressure improve. This is consistent with the idea that the best value for β for the cross-stream terms should be small because the cross-stream velocity is small. The pressure in the core, which depends primarily on the cross-stream velocity, shows a similar improvement. When β is very small, the pressure at the upstream plane behaves in a similar manner to the pressure in the CFX-TASCflow solutions (Figures 7–8) indicating that there is a comparatively large error introduced by the upstream boundary condition. This error is transferred, as in the CFX-TASCflow case, to a poor prediction for the velocity deficit in the core: Figures 22 and 23. While the mechanism for this loss of accuracy is not completely understood, it appears that the radial velocity at the upstream boundary is overpredicted. The overpredicted radial velocity is convected downstream and causes axial velocity to be convected away from the core resulting in an overprediction of the velocity deficit.

3 The evolution of a turbulent vortex

TRANSOM was also used to calculate the flow in a turbulent vortex using the Spalart-Allmaras turbulence model[5]. The kinematic viscosity, ν, was set to 10^{-6}, the circulation, C, to 0.1 and on the upstream plane the velocity was initialized to

$$v_\theta = \frac{C}{2\pi r} e^{-\frac{r^2}{4}} \tag{17}$$

This yields the same initial velocity values as in the laminar case.

The Spalart-Allmaras viscosity, $\tilde{\nu}$, which is the independent variable in the turbulence model, was initialized to

$$\tilde{\nu} = 10^{-3} e^{-\frac{r^2}{4}} \tag{18}$$

in the upstream plane. Therefore the turbulent viscosity at the core is similar to the laminar viscosity in the previous runs, but falls off exponentially with r at the same rate as the velocity.

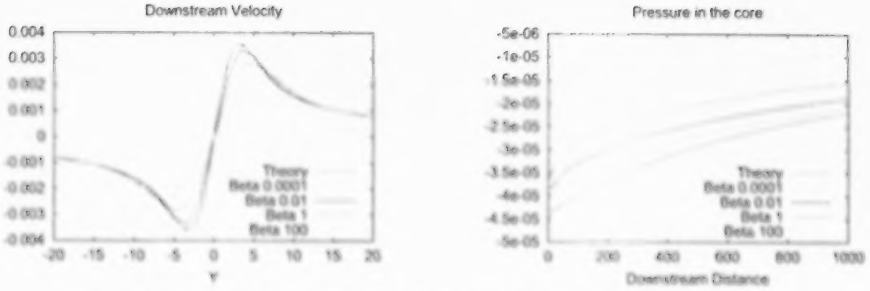

Figure 20: *Solutions with β varying from 0.0001 to 100; three cells across the core.*

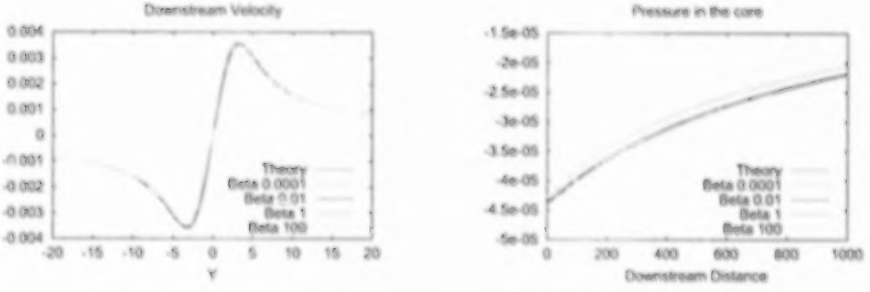

Figure 21: *Solutions with β varying from 0.0001 to 100; six cells across the core.*

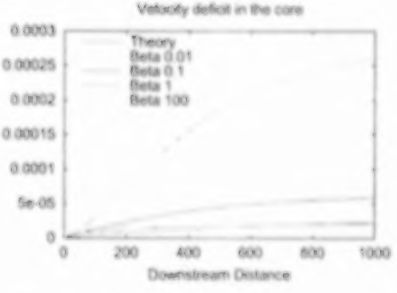

Figure 22: *Velocity deficit in the core with β varying from 0.01 to 100; three cells across the core.*

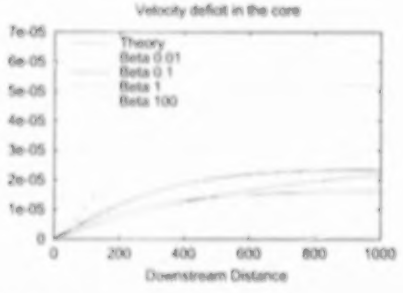

Figure 23: *Velocity deficit in the core with β varying from 0.01 to 100; six cells across the core.*

For this flow there is no analytic solution so the purpose was to test the sensitivity of the turbulence model to the grid and to TRANSOM input parameters. In all runs the flux difference order for the momentum and continuity equations was five and the pseudo-compressibility constant, β, was 1.0.

TRANSOM implements two versions of the Spalart-Allmaras turbulence model, one based on weak conservation forms of the equations, and the second based on an (almost) strong formulation (one term in the Spalart-Allmaras equations cannot be cast into a strong conservation form). In the weak version, the convective terms are constrained to be first order; in the strong version they may be first, third or fifth order.

Figures 24–26 compare the results of the turbulent calculations with varying numbers of cells across the vortex core. In all runs the strong version of the turbulence model was used with flux difference order of three.

In comparison with the laminar solutions, the turbulent solutions are somewhat more sensitive to the number of cells in the core. With three cells across the core the pressure is underpredicted at the downstream plane by about 40% (in the laminar case it was 30%); with six cells by about 10% (laminar was 6%). Since the pressure drop varies with the square of the velocity, if used to predict cavitation inception, an error of 10% in pressure would translate to an error in inception speed of about 5%: about a knot for typical naval vessels.

Figures 27 and 28 compare the solutions from the strong version of the turbulence model with varying order of the convective terms. The number of cells across the vortex core was six. The first order solution underpredicts the turbulent viscosity significantly, but this has a small effect on the velocity and pressure. In fact, the effect on the velocity was so small that it has not been shown. On the other hand, there is very little difference between the third order and fifth order solutions, even for the turbulent viscosity.

The solutions from the weak version and the strong version with first order convective terms are compared in Figures 29 and 30. In both cases the convective terms were first order (the only possibility for the weak version). The turbulent viscosity in the downstream plane agrees to within 2%. This discrepancy has a barely discernible effect on the velocity and pressure. It is much less important than the effect of higher flux difference order in the strong version.

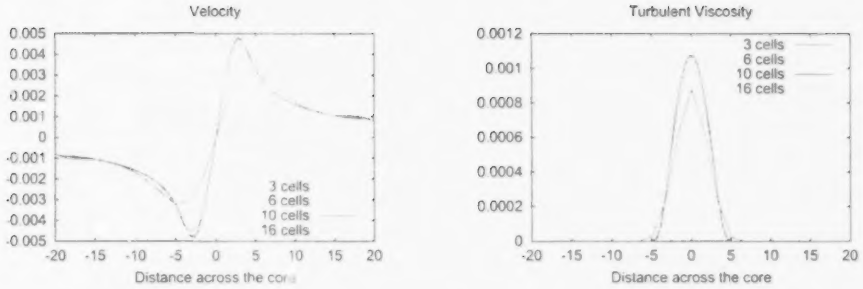

Figure 24: *Turbulent vortex: velocity and turbulent viscosity in the downstream plane.*

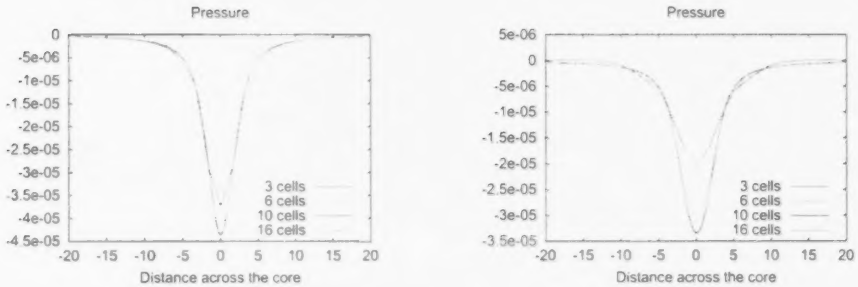

Figure 25: *Turbulent vortex: pressure in the upstream and downstream planes.*

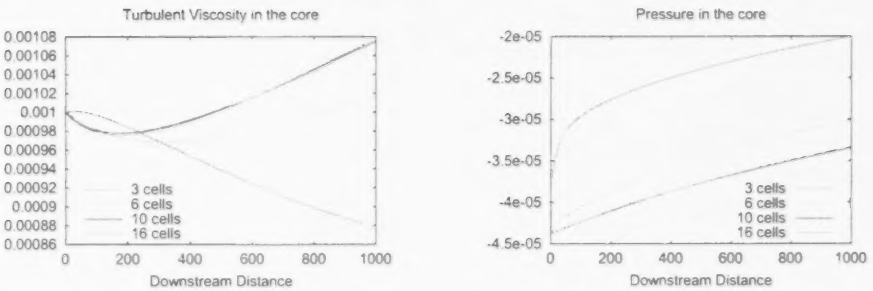

Figure 26: *Turbulent vortex: turbulent viscosity and pressure in the vortex core.*

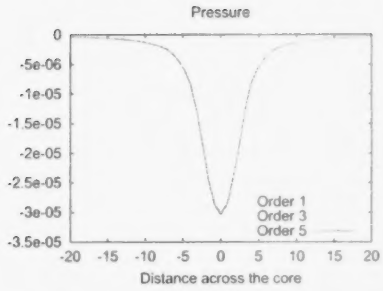

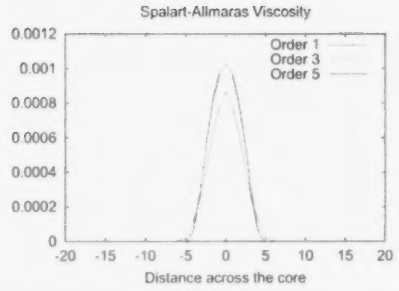

Figure 27: *The effect of the order of the turbulence model convective terms: Pressure and turbulent viscosity at the downstream plane.*

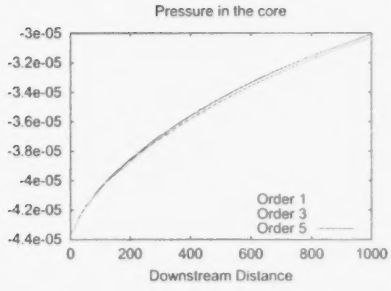

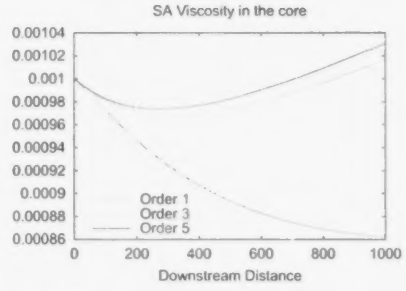

Figure 28: *The effect of the order of the turbulence model convective terms: Pressure and turbulent viscosity in the vortex core.*

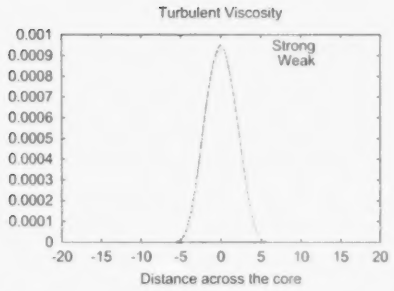

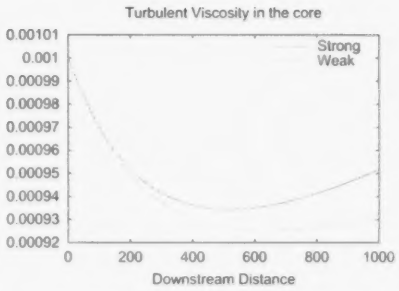

Figure 29: *Turbulent viscosity at the downstream plane.*

Figure 30: *Turbulent viscosity in the vortex core.*

4 Concluding remarks

Both TRANSOM and CFX-TASCflow generated accurate solutions for the laminar vortex, even when the grid density was very sparse. For practical purposes it appears that five or six cells across the core is the minimum necessary to model the pressure in the core adequately for the purposes of cavitation inception (error in inception speed less than one knot). Ten cells across the core would be preferred.

The TRANSOM solutions using first order convective terms are completely inadequate; the vortex decays very quickly. The third order solutions are much better but for comparable accuracy with the fifth order solutions at least three times the number of cells across the core are needed. The fifth order solutions are clearly to be preferred.

The TRANSOM solutions showed considerable variability with the pseudo-compressibility constant, β, though this is partially due to the large difference in velocity scales along different coordinate directions in the grid. There seems no need to alter the rule of thumb that β should be set to the square root of a typical velocity.

The turbulent solutions showed greater sensitivity to the grid density than the laminar solutions. However, the pressure and velocity predictions were comparatively insensitive to the order of the convective terms in the turbulent transport equation. Using first order convective terms is probably adequate for most purposes; when higher accuracy is required third order can be used. There was no discernible difference in the accuracy of the third and fifth order solutions.

The different implementations of the Spalart-Allmaras turbulence model used by TRANSOM were also found to give similar results.

References

1. Hally, D. (1997). TRANSOM: A Multi-method Navier-Stokes Solver: Overall Design. (DREA TM 97-231). Defence R&D Canada – Atlantic.

2. CFX-TASCflow (Online). AEA Technology Ltd. `http://www.software.aeat.com/cfx/products/cfx-tascflow` (Apr. 2002).

3. Batchelor, G. K. (1967). An Introduction to Fluid Mechanics, Cambridge University Press. Page 204.

4. Waterloo Maple Web Site (Online). Waterloo Maple Inc. `http://www.maplesoft.com` (April 2002).

5. Spalart, P. R. and Allmaras, S. R. (1992). A One-Equation Turbulence Model for Aerodynamic Flows. Technical Report. AIAA Paper 92-0439.

Distribution List

CANADA

Internal

1 Author

5 Library

Department of National Defence

National Defence Headquarters
MGen. George R. Pearkes Bldg.
101 Colonel By Drive
Ottawa, Ontario
K1A OK2

1 DRDCIM

2 DMSS 2

Others

2 Canada Institute for Scientific and Technical Information
Library Serials Acquisitions
National Research Council Canada
Ottawa, Ontario
K1A OS2

2 Canadian Acquisitions Division
National Library of Canada
395 Wellington Street
Ottawa, Ontario
K1A ON4
Attn: Government Documents

1 Director-General
Institute for Marine Dynamics
National Research Council of Canada
P.O. Box 12093, Station A
St. John's, Newfoundland
A1B 3T5

1 Director-General
Institute for Aerospace Research
National Research Council of Canada
Building M-13A
Ottawa, Ontario
K1A OR6

1 Transport Development Centre
Transport Canada
6th Floor
800 Rene Levesque Blvd, West
Montreal, Que.
H3B 1X9
Attn: Marine R&D Coordinator

1 Canadian Coast Guard
Ship Safety Branch
Canada Building, 11th Floor
344 Slater Street
Ottawa, Ontario
K1A 0N7
Att: Chief, Design and Construction

MOUs

11 Canadian Project Officer ABC-17 (H/WSS, DREA)

USA

1 Commanding Officer
U.S. Coast Guard Research and Development Center
1082 Shennecosett Road
Groton, CT 06340-2602
USA

THE NETHERLANDS

2 Ministry of Defence
Director of the Department of Naval Architecture and Marine Engineering
P.O. Box 20702
2500 ES The Hague
The Netherlands

1 Maritime Research Institute Netherlands
P.O. Box 28
6700 AA Wageningen
The Netherlands
Attn: Head Naval Research

AUSTRALIA

1 Department of Defence (Navy Office) Campbell Park Office CPI-505
Canberra ACT 2600
Australia
Attn: Director Naval Ship Design

DOCUMENT CONTROL DATA

(Security classification of title, body of abstract and indexing annotation must be entered when document is classified)

1 ORIGINATOR (the name and address of the organization preparing the document. Organizations for whom the document was prepared, e.g. Centre sponsoring a contractor's report, or tasking agency, are entered in section 8.)

Defence R&D Canada – Atlantic
PO Box 1012, Dartmouth, NS, Canada B2Y 3Z7

2 SECURITY CLASSIFICATION (overall security classification of the document including special warning terms if applicable).

UNCLASSIFIED

3 TITLE (the complete document title as indicated on the title page. Its classification should be indicated by the appropriate abbreviation (S,C,R or U) in parentheses after the title).

RANS calculations of the evolution of vortices

4 AUTHORS (Last name, first name, middle initial. If military, show rank, e.g. Doe, Maj. John E.)

Hally, David ; Watt, George D.

5 DATE OF PUBLICATION (month and year of publication of document)	6a. NO. OF PAGES (total containing information. Include Annexes, Appendices, etc).	6b. NO. OF REFS (total cited in document)
May 2002	19	5

7 DESCRIPTIVE NOTES (the category of the document, e.g. technical report, technical note or memorandum. If appropriate, enter the type of report, e.g. interim, progress, summary, annual or final. Give the inclusive dates when a specific reporting period is covered)

Technical Report

8 SPONSORING ACTIVITY (the name of the department project office or laboratory sponsoring the research and development. Include address).

Defence R&D Canada – Atlantic
PO Box 1012, Dartmouth, NS, Canada B2Y 3Z7

9a. PROJECT OR GRANT NO. (if appropriate, the applicable research and development project or grant number under which the document was written. Specify whether project or grant).	9b. CONTRACT NO. (if appropriate, the applicable number under which the document was written)
11de11	

10a. ORIGINATOR'S DOCUMENT NUMBER (the official document number by which the document is identified by the originating activity. This number must be unique.)	10b. OTHER DOCUMENT NOs. (Any other numbers which may be assigned this document either by the originator or by the sponsor.)
DREA TR 2001-216	

11 DOCUMENT AVAILABILITY (any limitations on further dissemination of the document, other than those imposed by security classification)

(X) Unlimited distribution
( ) Defence departments and defence contractors; further distribution only as approved
( ) Defence departments and Canadian defence contractors; further distribution only as approved
( ) Government departments and agencies; further distribution only as approved
( ) Defence departments; further distribution only as approved
( ) Other (please specify):

12 DOCUMENT ANNOUNCEMENT (any limitation to the bibliographic announcement of this document. This will normally correspond to the Document Availability (11). However, where further distribution beyond the audience specified in (11) is possible, a wider announcement audience may be selected).

13 ABSTRACT (a brief and factual summary of the document. It may also appear elsewhere in the body of the document itself. It is highly desirable that the abstract of classified documents be unclassified. Each paragraph of the abstract shall begin with an indication of the security classification of the information in the paragraph (unless the document itself is unclassified) represented as (S), (C), (R), or (U). It is not necessary to include here abstracts in both official languages unless the text is bilingual)

The evolution of a laminar vortex was calculated using the Reynolds-averaged Navier-Stokes solvers TRANSOM and CFX-TASCflow. Calculations were done on grids of varying density and were compared to an approximate solution of the Navier-Stokes equation. Both solvers generated accurate predictions for this flow. The solutions were used to make recommendations for the grid density required for accurate predictions of the pressure in the core as the vortex evolves over hundreds of core diameters.

TRANSOM was also used to determine the effect of grid density on a turbulent vortex, though in this case there is no analytic solution for comparison.

14 KEYWORDS, DESCRIPTORS or IDENTIFIERS (technically meaningful terms or short phrases that characterize a document and could be helpful in cataloguing the document. They should be selected so that no security classification is required. Identifiers, such as equipment model designation, trade name, military project code name, geographic location may also be included. If possible keywords should be selected from a published thesaurus, e.g. Thesaurus of Engineering and Scientific Terms (TEST) and that thesaurus-identified. If it not possible to select indexing terms which are Unclassified, the classification of each should be indicated as with the title).

Computational fluid dynamics
Fluid flow
Vortex flows
Turbulence
Spalart-Allmaras turbulence model
TRANSOM
CFX-TASCflow